Magnetically Tunable Band-Stop Filters

GEORGE L. MATTHAEI, FELLOW, IEEE

Abstract—Techniques for the design of magnetically tunable band-stop filters using ferrimagnetic garnet resonators (such as yttrium-iron-garnet spheres) are presented. Design for prescribed response, starting from a low-pass lumped-element prototype filter is outlined. The filter structure consists of a strip line or waveguide with garnet spheres mounted at intervals of approximately a one-quarter-wavelength or three-quarters-wavelength, at the center of the tuning range. Tuning is achieved by varying a biasing magnetic field. Techniques for enhancing the coupling to the garnet-sphere resonators are discussed, and the results of four trial designs which verify the theory are presented. The band-stop filter techniques are shown to also provide a very simple means for measuring the ferrimagnetic resonance linewidth ΔH of garnet spheres.

I. General

MAGNETICALLY tunable band-stop filters are of interest for applications where it is desired to blank out an interfering signal, using electronic control to adjust the blanking frequency. One possible application for this type of device is in combination with a swept-frequency superheterodyne receiver. A narrow-band, magnetically tunable band-stop filter could be used to eliminate the image response of such a receiver. As the receiver operating band is swept, the stop band of the filter could also be swept so as continuously to eliminate the image response.

The resonators of the filters under discussion use ferrimagnetic resonance in spheres of such material as single-crystal, yttrium-iron-garnet (YIG) [1]. In YIG resonators, the resonant frequency can be controlled by varying a biasing, dc magnetic field [1], [2]. Figure 1 shows a typical band-stop filter response [3] obtainable using ferrimagnetic resonators. Note that a small spurious response is indicated. Such responses result from higher-order magnetostatic-mode resonances, as occur from nonuniformities in the dc or RF fields within the resonator spheres.

Figure 2 shows one form of strip-line band-stop filter, which can be tuned by varying the biasing field strength H_0. The filter shown uses three YIG resonators, each of which is magnetically coupled to the strip-line center conductor. Figure 3(a) shows an equivalent circuit for a ferrimagnetic resonator with its magnetic coupling to the transmission line. In the vicinity of resonance, the circuit in Fig. 3(a) can be replaced by the circuit shown in Fig. 3(b). Thus, in the vicinity of resonance, the filter in Fig. 2 may be viewed as having three anti-resonant circuits connected in series with lines approximately a quarter-wavelength long.

Figure 4 shows a waveguide version of the filter in Fig. 2. In this design, the region in which the YIG spheres are located uses reduced-height guide in order to increase the coupling to the YIG resonators. Step transformers are used at the ends of the reduced-height section in order to provide a good impedance match. In some cases, it may be necessary to space the spheres by approximately three-quarters-wavelength instead of one-quarter-wavelength, in order to avoid direct coupling *between* spheres.

Figure 5 shows another form of strip-line band-stop filter structure to be treated herein. In this case, part of the center conductor is replaced by a low-pass filter structure consisting of sections of high- and low-impedance transmission lines, which simulate series inductances and shunt capacitances, respectively [4], [5]. This configuration makes possible a more compact structure, so that smaller magnet pole faces can be used. It will be shown that this form of structure permits tighter coupling to the resonators (which will result in a broader stop-band width and higher midstop-band attenuation). A similar effect can be obtained in waveguide by using a corrugated waveguide filter structure [5], [6].

It will be shown that another way of increasing the coupling to the ferrimagnetic resonators is to use dielectric loading in a structure such as that in Fig. 2. For a given line impedance, the higher the relative dielectric constant of the surrounding medium, the tighter the coupling can be. (However, other practical considerations will limit how far this can be carried.)

Kotzebue [7] has discussed certain aspects of reciprocal band-stop YIG filters of the forms in Figs. 2 and 4, and has also constructed nonreciprocal waveguide band-stop YIG filters. Herein we will present general design theory for reciprocal band-stop filters of the forms in Figs. 2, 4, and 5 expressed in the viewpoint of Young, Matthaei, and Jones [3]. The theory will then be compared with experimental results.

II. Band-Stop Filter Design Equations

A quarter-wave-coupled band-stop filter (analogous to the filter in Fig. 2) using resonators of the form in Fig. 3(b) is shown in Young, et al. [3], Fig. 4. The design equations necessary for the design of the filter from a low-pass prototype [8] are also given. The resonators of the filter are characterized by their resonant frequency ω_0 (which is the same for all of the resonators) and their *susceptance slope parameter* b_1. The suscep-

Manuscript received August 10, 1964; revised December 4, 1964. This research was sponsored by the U. S Army Electronics Research and Development Lab., Ft. Monmouth, N. J., under Contract DA 36-039 AMC-00084(E).

The author is with the Department of Electrical Engineering, University of California, Santa Barbara, Calif. He was formerly with Stanford Research Institute, Menlo Park, Calif.

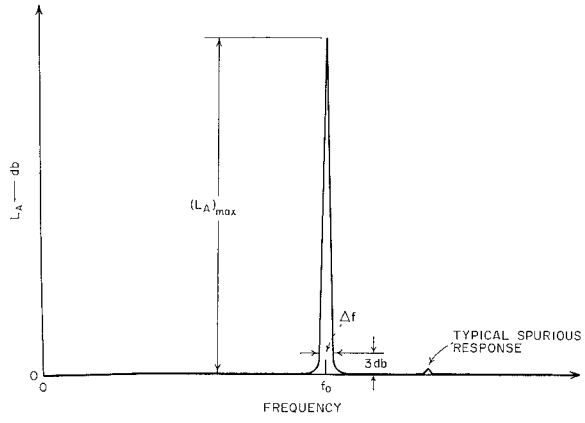

Fig. 1. Definition of band-stop filter response parameters.

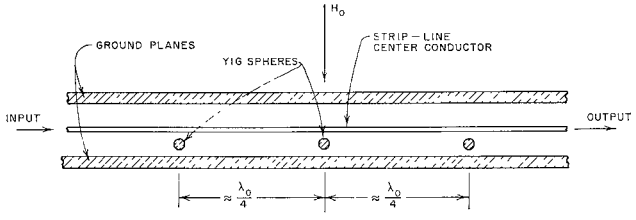

Fig. 2. A magnetically tunable strip-line band-stop filter.

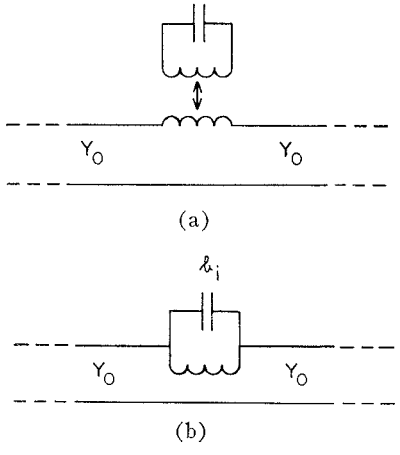

Fig. 3. Equivalent circuits of a YIG sphere coupled to a strip line or waveguide as shown in Figs. 2 and 4. (In this figure, resonator loss are neglected.)

tance slope parameter of a resonator is defined as

$$b_1 = \frac{\omega_0}{2} \frac{dB_1}{d\omega}\bigg|_{\omega=\omega_0} \tag{1}$$

where B_i is the susceptance of the resonator. Note that b_i has the dimensions of susceptance; for a lumped-element resonator such as that in Fig. 3(b), $b_i = \omega_0 C_i$, where C_i is the capacitance of the capacitor. Equation (1), however, applies regardless of the form of the resonator, as long as the resonator exhibits a parallel-type of resonance (i.e., $B_i = 0$ at resonance). If a resonator with a slope parameter of b_i is shunted by a conductance G_i, the Q of the combination is

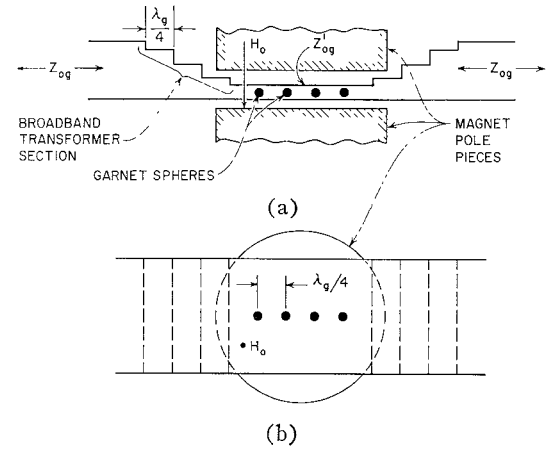

Fig. 4. A four-resonator magnetically tunable waveguide band-stop filter. (a) Side view. (b) Top view.

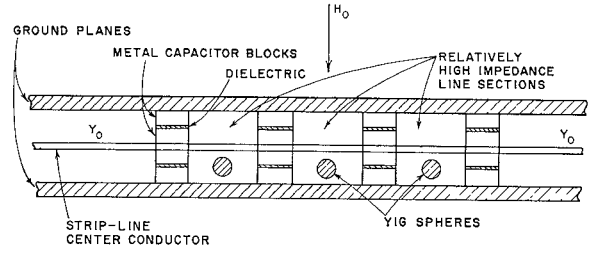

Fig. 5. A suggested magnetically tunable band-stop filter configuration that permits increased coupling to the YIG spheres.

$$Q_i = \frac{b_i}{G_i} \tag{2}$$

Equation (1) of Young, et al. can be used to map low-pass prototype filter responses [8] so as to find the number of resonators required to give the desired rate of cutoff, along with the desired form of pass band characteristic. After a suitable low-pass prototype filter has been selected, the susceptance slope parameters required for the resonators of the band-stop filter can be computed in normalized form using Fig. 4 of Young, et al. For simplicity and practicality, it is convenient in Fig. 4 of Young, et al., to use $Y_0 = Y_1 = Y_2 = \cdots = Y_{n-1}$ and to use low-pass prototypes [8] having $g_0 = g_{n+1}$. Chebyshev filters with n odd and all maximally flat filters satisfy this condition, provided that they are designed for minimum pass band reflection loss. After the required normalized resonator slope parameters are determined, the required ferrimagnetic resonator properties can be determined, as explained in Section III of this discussion.

Figure 8 of Young, et al., gives data from which the maximum attenuation $(L_A)_{max}$ of a band-stop filter can be computed from the unloaded Q of the resonators Q_u, the fractional stop-bandwidth w, and the low-pass prototype element values $g_0, g_1, \cdots, g_{n+1}$. A case of special interest is that where an equal-element prototype having $g_0 = g_1 = g_2 = \cdots = g_{n+1} = 1$ is used. This leads to a

band-stop filter having all of its resonators exactly the same. In this case, if the $Y_i = Y_0$, the equations in Fig. 4 of Young, et al., reduce to

$$\left.\frac{b_i}{Y_0}\right|_{i=1 \text{ ton}} = \frac{1}{\omega_1' w}, \tag{3}$$

and in Fig. 8 by Young, et al. [3].

$$(L_A)_{\max} = 20n \log_{10} (w\omega_1' Q_u) - 6\text{dB} \tag{4}$$

If ω_i' is defined as the 3-dB point of the low-pass prototype response, for equal-element prototypes with all $g_i = 1$, computations show that ω_1' varies with the number n of reactive elements as follows:

$$\begin{aligned} n &= 1 \quad \omega_1' = 2 & \qquad n &= 3 \quad \omega_1' = 1.52 \\ n &= 2 \quad \omega_1' = 1.41 & \qquad n &= 4 \quad \omega_1' = 1.65 \end{aligned} \tag{5}$$

Using ω_1' defined in this way, w is the fractional bandwidth $w = \Delta f/f_0 = (\omega_2 - \omega_1)/\omega_0$, where Δf is the bandwidth at the 3-dB points, as indicated in Fig. 1. It is interesting to note from (3) and (5) that, for a given resonator slope parameter for the resonator, adding one resonator so as to total two, will *increase* the 3-dB stop-bandwidth by a factor of $\sqrt{2}$, but from there on, adding more resonators with the same slope parameter will cause the 3-dB stop-bandwidth to become narrower.[1] However, adding more resonators will cause the peak attenuation $(L_A)_{\max}$ to be larger, and the bandwidth at, say, the 20- or 30-dB attenuation levels should be greater.

III. Determination of Ferrimagnetic-Resonator and Coupling-Structure Dimensions

If in Fig. 3(b) a short circuit is placed across the transmission line just to the right of the resonator, and if the line to the left of the resonator is terminated in a conductance $G = Y_0$, by (2) the circuit will be seen to have a Q of

$$(Q_e)_i = \frac{b_i}{Y_0} \tag{6}$$

The Q here has been designated Q_e, because this Q corresponds to what is commonly called the *external* Q of a resonator, i.e., the Q that a resonator would have if its internal losses were removed and it were loaded only by the external circuit to the left in Fig. 3(b). Note that $(Q_e)_i$ above is the same as the normalized resonator slope parameters in Fig. 4 of Young, et al., and in (3) herein. Thus, we shall find that existing data for determining the external Q of YIG resonators in short-circuited, strip-line, and waveguide structures will prove very useful in band-stop filter design, as well as in the determination of the linewidth of ferrimagnetic crystals (a subject to be discussed in Section V). The short-circuit condition imposed to obtain (6) is, of course, hypothetical as far as band-stop filters are concerned. But imposing this hypothetical short circuit provides a convenient way for establishing the b/Y_0 ratio of a YIG resonator coupled to a line.

P. S. Carter, Jr. [2] has derived equations for the external Q of YIG ferrimagnetic resonators in strip-line and in waveguide structures and has also prepared easy-to-use charts for certain cases [9]. Carter's charts [9] are reproduced in Figs. 6 and 7. The chart in Fig. 6 gives the external Q of a YIG-sphere ferrimagnetic resonator in a 50-ohm strip-line structure, where the sphere is assumed to be placed close to a short circuit in the structure, or at some multiple of a half-wavelength from the short circuit. Figure 6 gives Q_e for given sphere diameter D_m and strip-line to ground-plane spacing d, both in inches. The chart given applies specifically to a 50-ohm strip line and to YIG (which has a saturation magnetization of $4\pi M_s = 1750$ gauss). This chart can be adapted for use in other situations by use of the formula

$$Q_e = (Q_e)_{\text{chart}} \frac{50}{Z_0'} \left(\frac{Z_0}{Z_0'}\right) \left(\frac{1750}{4\pi M_s}\right) \frac{1}{\epsilon_r} \tag{7}$$

where $(Q_e)_{\text{chart}}$ is the value of Q_e obtained from Fig. 6 for the given values of d and D_m, Z_0' is the actual characteristic impedance of the strip line to which the ferrimagnetic sphere is coupled, $4\pi M_s$ is the saturization magnetization of the ferrimagnetic material in gauss, and ϵ_r is the relative dielectric constant of the medium surrounding the strip line. The impedance Z_0 indicated in the formula will now be explained.

As mentioned in Section I, the filter in Fig. 5 utilizes a low-pass filter structure having sections of high-impedance line to simulate series inductances, and sections of low-impedance lines to simulate shunt capacitances. Such structures can be designed on the image basis [4], from lumped-element filter prototypes [5], [8,] or from step-transformer prototypes [5], [10]. In the pass band of this filter, the structure can be viewed as operating like an artificial transmission line of *image* impedance $Z_0 = 1/Y_0$, which corresponds to the characteristic impedance Z_0 of the uniform strip line in Fig. 2. However, though the effective line impedance that the ferrimagnetic resonators observe is Z_0, the resonators are actually coupled to short line sections of much higher impedance Z_0'. Thus, if $Z_0 = 50$ ohms while $Z_0' = 100$ ohms, the resulting Q_e value will be $(50/100)^2 = 0.25$ times what it would be if the sphere were coupled to a uniform 50-ohm line (case of $Z_0 = 1/Y_0 = Z_0' = 50$). This Q_e value of one-fourth the size corresponds to a considerably tighter coupling between the line and the sphere, and would result in a broader stop-bandwidth and higher peak attenuation $(L_A)_{\max}$.

[1] This neglects the effect of dissipation loss which will tend to broaden the 3-dB bandwidth as the number of resonators is increased.

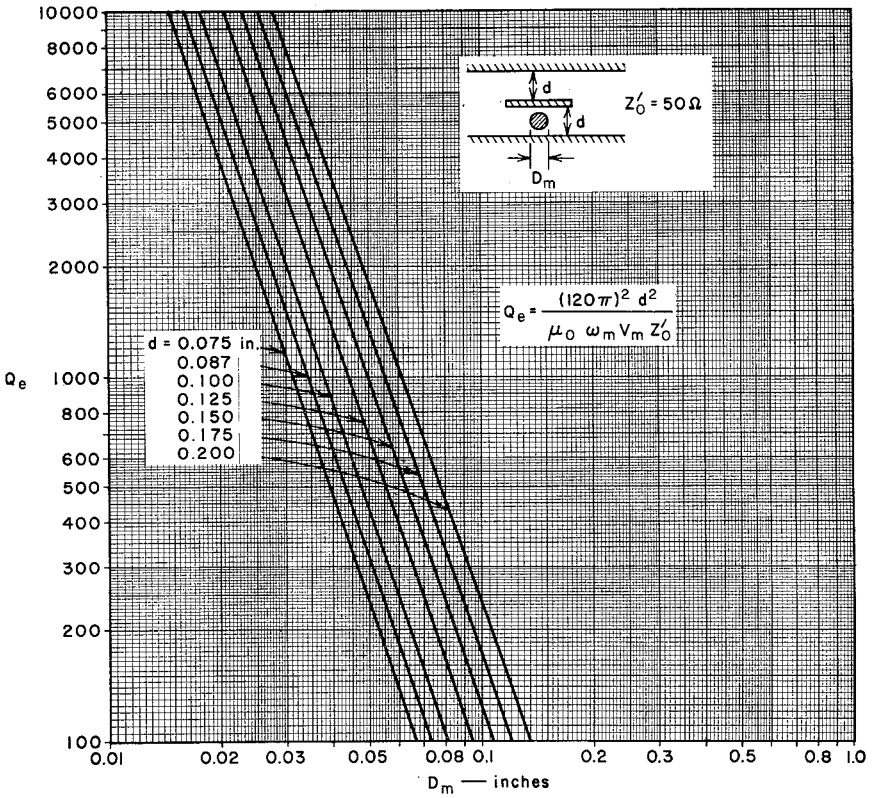

Fig. 6. Carter's chart of Q_e vs. sphere diameter for a spherical YIG resonator in short-circuited, symmetrical strip transmission line.

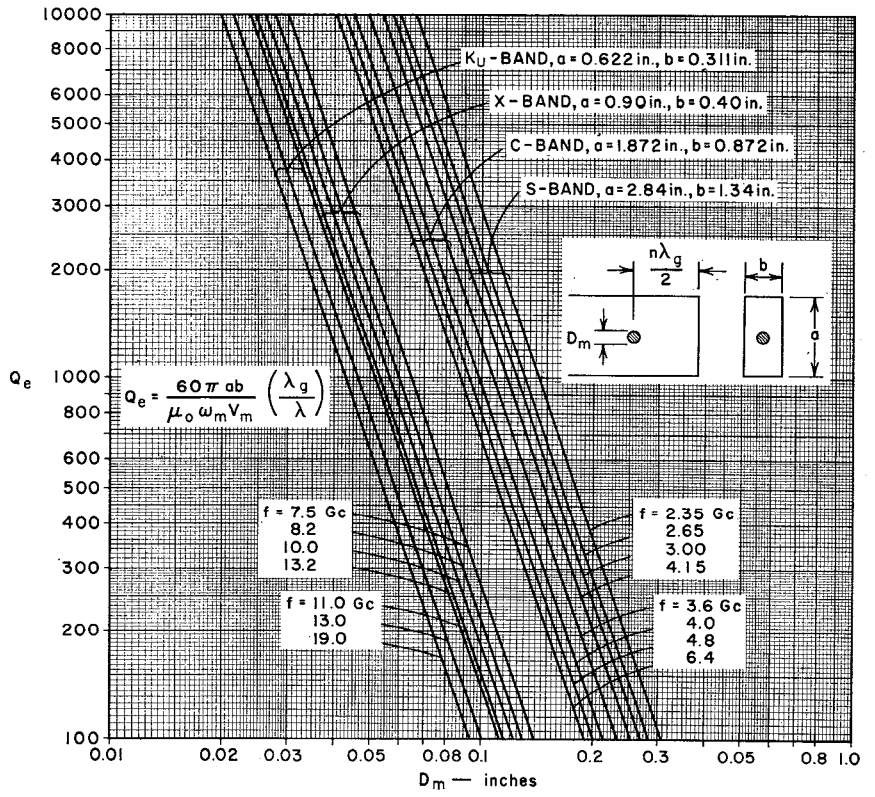

Fig. 7. Carter's Chart of Q_e vs. sphere diameter of spherical YIG resonator located at a high-current position in short-circuited TE_{10} rectangular waveguide.

Carter's chart in Fig. 6 was derived using a mathematical model, which assumed a strip line with no fringing capacitance. Thus, as the strip line becomes sufficiently narrow so that fringing effects influence the RF magnetic field seen by the sphere, the chart will become less accurate. Caution must also be taken in using too narrow a strip for coupling to the sphere because, if the RF magnetic field is very nonuniform, higher-order magnetostatic modes will be excited.

Figure 7 shows an analogous chart for a YIG sphere next to a short circuit (or a multiple of a half wavelength from a short circuit) in S-band, C-band, X-band, and KU-band standard rectangular waveguide. In this case (7) is replaced by[2]

$$Q_e = (Q_e)_{\text{chart}}\left(\frac{b'}{b}\right)\left(\frac{b''}{\sqrt{\epsilon_r}\,b'}\right)\left(\frac{1750}{4\pi M_s}\right) \cdot\left(\frac{\lambda}{\lambda_g}\right)_{\text{air}}\left(\frac{\lambda_g}{\lambda}\right)_{\text{diel}} \quad (8)$$

where b is the height of standard guide as indicated in Fig. 7, b' is the height of the guide actually used in the vicinity of the sphere, and b'' applies to the case where a corrugated waveguide structure is used [4], [5], [6] (which provides the analogous waveguide filter to the strip-line filter in Fig. 5). The waveguide height b'' is the height of guide that would have the same characteristic impedance as the corrugated waveguide structure. If the waveguide structure is not corrugated, $b'' = b'$. The parameter $(\lambda/\lambda_g)_{\text{air}}$ is the ratio of the plane-wave wavelength to guide wavelength for air, $(\lambda_g/\lambda)_{\text{diel}}$ is the reciprocal quantity for propagation in the dielectric, and the other parameters are as discussed previously.

IV. Experimental Results

Several experimental strip-line structures were fabricated in order to test the theory discussed above. Filter 1 had the following construction and parameters:

1) Physical form as in Fig. 2, with a 50-ohm strip line having a strip-line to ground-plane spacing of $d = 0.110$ inch (and a ground-plane to ground-plane spacing of 0.240 inch).
2) Two YIG-sphere resonators of diameter $D_m = 0.072$ inch located beneath the strip line and spaced 0.90 inch apart from center to center.

The YIG spheres were mounted on small dielectric rods, which could be rotated so as to tune both spheres to the same resonant frequency [11] (by adjusting the effect of the crystalline anisotropy field on the resonant frequency).

Table I shows the measured results obtained with Filter 1. For resonance at $f_0 = 2.0$ Gc/s, the biasing magnetic field is not sufficiently large to permit very good operation, but above approximately $f_0 = 2.2$ Gc/s the performance is reasonably good. Note that $(L_1)_{\max}$ is 32.0 dB for $f_0 = 3.0$ Gc/s and increases for larger values of f_0. The 3-dB bandwidth Δf (see Fig. 1) was measured,[3] and also computed using (3) and (5) for $n = 2$, (6), and Fig. 6 (which gave $Q_e \approx 170$). Note that except for the sizeable errors of $f_0 = 2.0$ Gc/s and $f_0 = 6.0$ Gc/s, which are believed to be due to the proximity of spurious responses, the agreement between computed and measured values of Δf is reasonably good. Since spurious responses (see Fig. 1) due to magnetostatic modes are always an important consideration in filters using ferrimagnetic resonators, the major spurious responses that were observed are noted on the right side of the table. These responses were observed by holding the signal frequency constant at the indicated value of f_0 while the biasing magnetic field was varied. Except at 2.0 Gc/s, which was out of the good operating range of the device (and possibly at 6.0 Gc/s, where there was a 1.4-dB high response), the spurious response activity was quite small.

It is well known that if a ferrimagnetic resonator has sufficient power incident upon it, it ceases to perform as a high-Q resonator. (This property is utilized in YIG limiters.) In the case of a band-stop filter, this means that the attenuation of the resonators will disappear if the incident power is large enough. Figure 8 shows the results of tests on Filter 1, which were made in order to determine the saturation characteristics of the filter. As expected, the attenuation dropped for a relatively small amount of incident power at 3000 Mc/s but no saturation was observed at 6000 Mc/s for the amount of power available from the signal generator being used. The low saturation level, which occurs in the vicinity of S band, is due to the fact that the spin-wave manifold for YIG overlaps the uniform-precessional mode in this frequency range, and nonlinear coupling sets in between the uniform-precessional mode and the spin-wave modes at quite low power levels [12]. Now the frequency range where there will be a large number of spin-wave modes with resonant frequencies which overlap that of the uniform precessional mode extends up to the frequency [12]

$$(f_0)_{\text{Mc/s}} = (\tfrac{2}{3})(2.8)(4\pi M_s) \quad \text{Mc/s} \quad (9)$$

(and somewhat beyond), where in this equation $4\pi M_s$ is in gauss. For YIG, which has $4\pi M_s = 1750$ gauss, (9) gives $(f_0)_{\text{Mc/s}} = 3270$ Mc/s. In order to prevent saturation effects from occurring at low power levels at S band, it is necessary to use a ferrimagnetic material such as gallium-substituted yttrium-iron-garnet (Ga-YIG),

[2] Note that here it is assumed that the guide width in the region of the dielectric is the same as is used where the guide is filled with air. Thus, here we have $\sqrt{\epsilon_r}$ instead of ϵ_r.

[3] In all the measured data in this section and in Section V, Δf was measured by interpolating from cavity wavemeter data using a swept signal generator and an oscilloscope. Thus the data for Δf are probably accurate to only plus or minus a few tenths of a megacycle.

TABLE I

MEASURED PERFORMANCE OF BAND-STOP FILTER NO. 1

(The filter had two resonators and was of the form in Fig. 2)

f_0 (Gc/s)	$(L_A)_{max}$ (dB)	Δf Measured (Mc/s)	Δf Computed (Mc/s)	Approx. H_0 (oersted)*	Major spurious responses
2.0	8.5	13.6†	8.3	730	2-dB high at $H=700$ oersted*
2.2	22.5	12.5	9.2	745	0.4-dB high at $H=520$ oersted*
3.0	32.0	15.2	12.5	1000	None observed
4.0	35.2	18.3	16.2	1450	0.1-dB high at $H=1510$ oersted*
5.0	36.8	19.4	20.3	1570	0.8-dB high at $H=1720$ oersted*
6.0	38.4	42.5†	24.3	1900	One, 1.4-dB high for $H=2090$ oersted. Another, 0.5-dB high for $H=2200$ oersted.*

* As measured approximately, with a gaussmeter of moderate accuracy.

† These oversized Δf values are believed to be due to the close proximity of spurious responses.

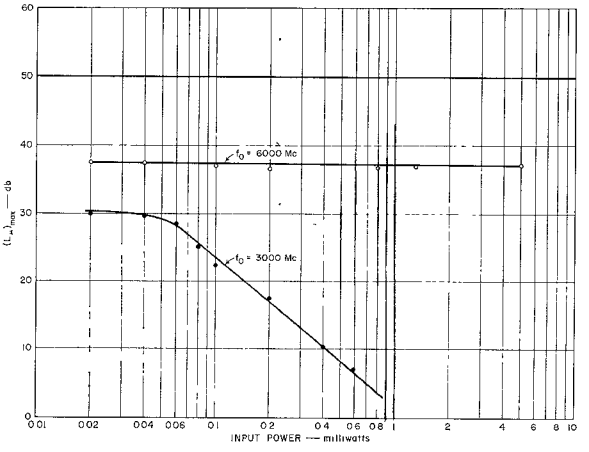

Fig. 8. $(L_A)_{max}$ vs. incident power for Filter 1.

which has a lower value of $4\pi M_s$. In the case of this particular device, no tests were made to determine the actual power levels for saturation at frequencies above S band. However, Carter [2], [13] found that in an X-band *band-pass* filter having a YIG resonator, 10 watts of incident power were required before saturation effects were apparent. In the case of an analogous X-band *band-stop* filter, saturation effects would be evident at a somewhat lower incident power level (estimates indicate at about a 6-dB lower power level), but the saturation effects would probably increase with power very gradually if the band-stop filter had multiple resonators. This is because the second band-stop resonator would not saturate until the attenuation of the first band-stop resonator was very low, so as to let most of the incident power by. Also, the tighter the coupling between the transmission line and the ferrimagnetic resonators (i.e., the smaller the b_2/Y_0), the larger will be the power handling ability of the filter. This is because as the resonator couplings get tighter, more power is reflected at resonance and less is absorbed by the resonators.

In order to test out the use of low-pass filter structures such as that in Fig. 5 for obtaining enhanced coupling, Filter 2 (shown in Fig. 9) was fabricated. This is a low-pass filter structure that was designed from a step-transformer prototype [10] as discussed in Section 7.06 of Matthaei, Young, and Jones [5], though other methods could also have been used. The structure of Filter 2 had the following properties:

1) A $Z_0=50$-ohm input line was followed by a low-pass structure consisting of a short section of $Z_0'=91$ ohm line, followed by a low-impedance section of 26 ohms impedance, followed by another section of $Z_0'=91$ ohms, followed by an output line of $Z_0=50$ ohms. The low-pass structure was designed to match $Z_0=50$ ohms in its pass band.
2) The cutoff frequency of the low-pass structure was 4000 Mc/s, so all desired signals should be below this frequency.
3) The two 91-ohm line sections were each 0.221 inch long, and the 26-ohm line section used Rexolite 1422 dielectric and was 0.139 inch long. The 50-ohm input and output line sections used Rexolite 1422 dielectric for rigidity.
4) Provision was made for mounting a YIG sphere on a rod at the center of each $Z_0'=91$-ohm line section. In order to reduce possible coupling between the two spheres, one sphere was mounted above, the other below its adjacent 91-ohm line section. The resonators were each mounted with a [110] crystal axis parallel to the mounting rod axis; the resonators were tuned by rotating the spheres about this axis (which was perpendicular to the biasing field H_0) [11].

When the filter was tested with two spheres, it was found that there was appreciable direct coupling between the spheres, in spite of efforts to avoid this difficulty. This coupling evidenced itself by interaction between the two spheres when either was tuned. Because of this, only one resonator could be used satisfactorily in this structure.

Tests were made on Filter 2 using one YIG sphere; Table II summarizes the results. Note that the measured and computed values of Q_e again agree reasonably well.

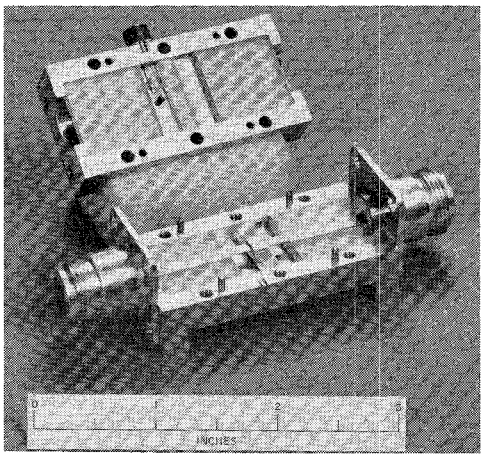

Fig. 9. Filter 2, which utilizes a low-pass filter structure to enhance the coupling between the main line and each YIG sphere.

TABLE II

MEASURED RESULTS OBTAINED ON THE FILTER STRUCTURE IN FIG. 9 USING ONE 0.072-INCH DIAMETER YIG RESONATOR

f_0 (Mc/s)	Δf (Mc/s)	$(L_A)_{max}$ (dB)	$Q_e \approx \frac{f_0}{2\Delta f}$	Q_e by (7)	Q_u
2200	26.2	11.8	42.0	49.0	283
3000	26.7	21.3	56.2	49.0	1039
4000	41.3	23.5	48.5	49.0	1460

The quantity on the right is the unloaded Q, Q_u. This was computed from the measured data by procedures to be discussed in Section V. Though the peak attenuation values were not quite as high as was expected, as was predicted by the theory the 3-dB stop-bandwidth values were increased to over three times the values which would be expected from the theory if this *single* resonator had been coupled to a uniform, air-filled 50-ohm line with the same center-conductor-to-ground-plane spacing.

In order for a filter structure such as Filter 2 to work satisfactorily with two or more spheres, the spheres could have been spaced so that the electrical distance between them is approximately $3\pi/2$ radians instead of $\pi/2$ radians in the operating range. This would make the direct coupling between resonators negligible, but this arrangement would also tend to limit further the tuning range over which full use of the resonators can be made. (If two identical band-stop resonators are separated by an odd multiple of $\pi/2$ radians, the total dB peak attenuation will be approximately twice the dB peak attenuation of either resonator alone. If two resonators are separated by a multiple of π radians, the total dB peak attenuation will be only about 5 dB more than that for one resonator alone.)

It appears probable that a multiresonator structure of the type in Fig. 5 could be designed to have adequate isolation between adjacent resonators if the shunt-capacitive sections of the structure were fabricated using metal shielding walls such as those to be discussed with regard to Filter 4 (Fig. 10). This type of shunt capacitor, plus arranging the resonators so they are alternately above and below the center conductor, would very likely give adequate isolation.

The low-pass filter structure in Fig. 9 was seen to give the desired increase in coupling as indicated by higher values of $(L_A)_{max}$, larger values of Δf, and approximately the predicted values of Q_e. It was, however, decided to also investigate the technique of surrounding the strip line with dielectric material in order to increase the coupling. In this case the increased coupling results from the fact that for a given line impedance Z_0', the larger ϵ_r, the narrower will be the strip line and the more the RF H-field will be concentrated in the region of the ferrimagnetic resonators.

The filter in Fig. 10 was first constructed without the metal shielding walls indicated in the figure. The first version which had a uniform center conductor with no shielding walls will be referred to as Filter 3, while the later version (shown in Fig. 10) which has metal shielding walls and a slightly notched center conductor will be referred to as Filter 4.

Filter 3 was designed and constructed using Rexolite 1422 (with $\epsilon_r = 2.55$) as the dielectric material. With $Z_0 = Z_0' = 50$ ohms, a 0.072-inch diameter YIG sphere, a ground-plane spacing of 0.240 inch, and a center conductor thickness of 0.020 inch, by (7) and Fig. 6 we find that $Q_e = 68.3$. For $Z_0 = Z_0'$ and the dimensions indicated above, we would have obtained $Q_e = 174$ if dielectric loading had not been used. Thus, the use of dielectric loading provides a very appreciable increase in coupling.

In the design of the structure for Filter 3 an effort was made to surround (as far as possible) the spheres with uniform dielectric material, while still providing means for rotating the spheres to achieve tuning. (Completely surrounding the sphere with dielectric material was felt to be important from the standpoint of avoiding serious trouble with magnetostatic modes caused by nonuniform RF fields.) A 0.091-inch diameter spherical cavity was machined out for each 0.072-inch diameter sphere in order to provide clearance. The spheres were cemented to Rexolite rods with their [110] crystal axis parallel to axis of the rod. With the mechanical arrangement shown in Fig. 10, it was possible to rotate the spheres for tuning while keeping them accurately positioned. The arrangement used also made it easy to remove a sphere and its rod if desired. The spheres in this structure were spaced 0.595 inches apart, which in the medium of this structure is a quarter wavelength at 3.1 Gc/s.

Tests were made on Filter 3 in the vicinity of 2200, 3000, 4500 Mc/s. For fixed dc magnetic field values, the

responses shown in Fig. 11 were obtained. Note that the responses have two peaks of attenuation instead of just one. This is due to a small amount of direct magnetic coupling between the two spheres, and it was not possible to eliminate these two peaks no matter how the resonators were tuned (i.e., by tuning, the peaks could be made to move further apart, but it was not possible to force them to merge into one peak). It was thought that the 0.595-inch spacing between the spheres would reduce this direct coupling to a negligible amount, but these responses show that this was not the case. This double-peaked form of response was not desired in this case, but it could be useful for some applications. It is interesting to note that the response in the vicinity of 2200 Mc/s in Fig. 11 is skewed towards the lower edge of the band, the response in the vicinity of 3000 Mc/s is nearly symmetrical, while the response at 4500 Mc/s is skewed towards the upper side of the band. This effect may be due to the fact that at 2200 Mc/s the spacing between the resonators is less than a quarter wavelength, at 3000 Mc/s it is almost exactly a quarter wavelength, while at 4500 Mc/s the spacing between spheres is greater than a quarter wavelength.

Filter 4 (shown in Fig. 10) is the same as Filter 3 except for a modification made in the center of the structure in order to eliminate, for practical purposes, all direct coupling between the YIG resonators. The brass center conductor of the structure was reduced in width to 0.090 inch over a 0.200-inch-long section, as shown in the figure. The dielectric material was removed from a 0.095-inch wide transverse section, and sliding metal walls were inserted. Reducing the width of the center conductor over the 0.200-inch section together with removing the section of dielectric, tended to leave the transmission line with a shortage of shunt capacitance throughout its center region (i.e., a shortage of shunt capacitance per unit length with respect to that required for a 50-ohm line). This shortage of capacitance was compensated for by sliding the metal shielding walls in toward the center conductor until the proper shunt capacitance was regained. The proper position of the shielding walls was determined by VSWR measurements made in the 2- to 4-Gc/s range. When the walls were spaced 0.130 inch apart, a very low VSWR was obtained across the entire operating range. By this technique, metal shielding walls were introduced that did not degrade the impedance characteristics of the structure, but that provided excellent RF shielding between the YIG spheres.

Table III summarizes the significant features of the response of band-stop Filter 4 at several operating frequencies. In this case, the stop band has only one attenuation peak, indicating that the direct coupling between resonators has been reduced to an insignificant amount. As is to be expected, the peak attenuation $(L_A)_{\max}$ increases with frequency, and by 4500 Mc/s it reaches a very high level, which is in excess of the 55 dB maximum

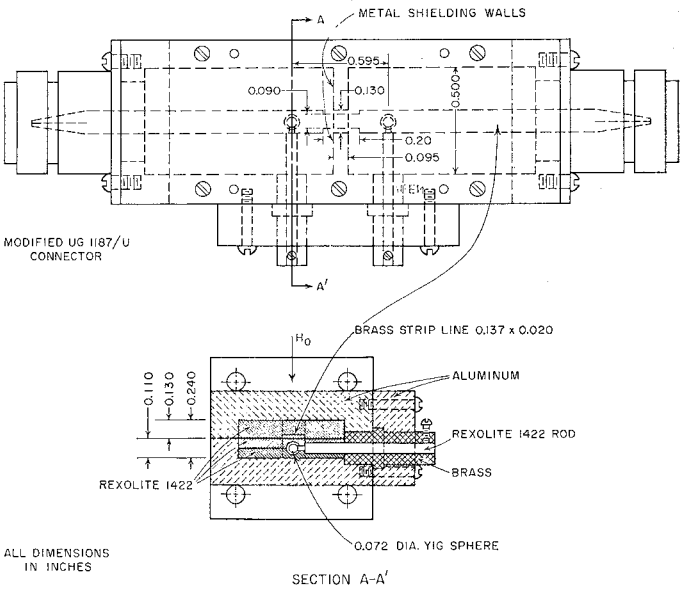

Fig. 10. Magnetically tunable band-stop Filter 4. (Filter 3 is same structure without metal shielding walls and with a uniform center conductor).

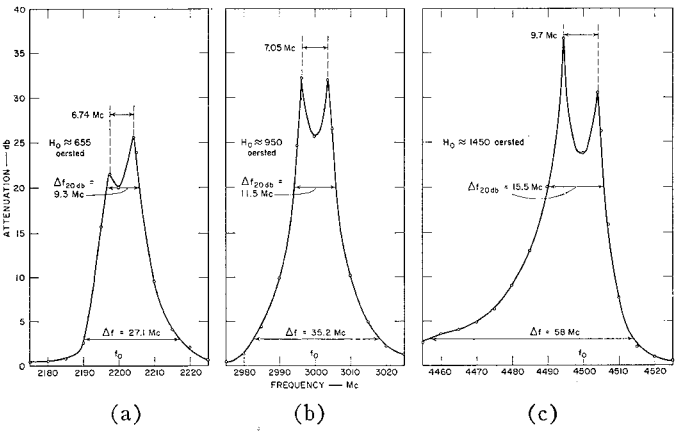

Fig. 11. Measured performance of the Filter 3 (which did not have the shielding walls indicated in Fig. 10).

attenuation that could be measured by the detection system being used. Also shown in Table III are the various spurious responses that were noted as the frequency was held constant and the biasing magnetic field varied. It appears likely that the indicated amount of spurious response activity would not be objectionable for most applications of interest.

Table IV shows the theoretical 3-dB and 20-dB bandwidths computed for Filter 4, along with the corresponding measured bandwidths. The agreement is seen to be very satisfactory. Also shown are the corresponding bandwidths for Filter 3 (which had double-peaked attenuation characteristics). As is to be expected, Filter 3 consistently had somewhat larger bandwidths than does Filter 4, because of the bandwidth broadening caused by the double peaks in the attenuation characteristic of Filter 3.

TABLE III

MEASURED RESPONSE PARAMETERS FOR BAND-STOP FILTER 4 SHOWN IN FIG. 10

f_0 (Mc/s)	$(L_A)_{max}$ (dB)	Δf (Mc/s)†	$\Delta f_{20\ dB}$ (Mc/s)†	H (Oersted)*§	Spurious response height (dB)*
2200	31.5	25.80	7.90	560	—
				400	1.0
				765	0.4
				835	0.3
3000	42.8	30.10	10.4	930	—
				840	0.2
				1050	0.7
				1170	0.1
4500	>55.5 (Limit of Detection)	43.40	11.2	1440	—
				1350	0.4
				1500	2.3
				1670	0.4

* Measured with the frequency held constant at the given f_0 value.

† Δf is the bandwidth at the 3-dB attenuation points and $\Delta f_{20\ dB}$ is the bandwidth at the 20-dB attenuation points.

§ As measured with a commercial gaussmeter of only moderate accuracy.

TABLE IV

COMPARISON OF THE MEASURED BANDWIDTHS FOR FILTERS 3 AND 4 WITH THE THEORETICAL BANDWIDTHS FOR A SINGLE-PEAKED RESPONSE

Theoretical bandwidths			Measured bandwidths for Filter 4		Measured bandwidths for Filter 3 (having double-peaked response)	
f_0 (Mc/s)	Δf (Mc/s)	$\Delta f_{20\ dB}$ (Mc/s)	Δf (Mc/s)	$\Delta f_{20\ dB}$ (Mc/s)	Δf (Mc/s)	$\Delta f_{20\ dB}$ (Mc/s)
2200	22.9	7.3	25.8	7.9	27.1	9.3
3000	31.2	9.9	30.1	10 4	35.2	11.1
4500	47.0	14.9	43.4	11.2	58.0	15.5

Δf = Bandwidth between 3-dB attenuation points.
$\Delta f_{20\ dB}$ = Bandwidth between 20-dB attenuation points.

V. A Simple Procedure for Measuring the Linewidth of Garnet Resonators

Operating a garnet sphere as a single resonator band-stop filter provides a simple means for determining the resonance linewidth ΔH of the garnet material. We shall now describe the necessary equations and procedures.

The effect of the internal loss in a garnet resonator in a band-stop filter can be represented by a conductance G_s in parallel with the L and C in Fig. 3(b). Then the unloaded Q of such a resonator is $Q_u = b/G_s$, where b is the resonator susceptance slope parameter. Using this definition of Q_u, along with $Q_e = b/Y_0$, by straightforward circuit analysis it is easily shown that, for a single-resonator band-stop filter,

$$Q_u = 2Q_e(A - 1) \tag{10}$$

where

$$A = \text{antilog}_{10}\frac{(L_A)_{max}}{20} \tag{11}$$

and $(L_A)_{max}$ was defined in Fig. 1. Now Q_u can also be expressed as

$$Q_u = \frac{H_0}{\Delta H} \tag{12}$$

where H_0 is the dc biasing field strength at resonance, and ΔH is the resonance linewidth [1]. Neglecting the effect of the anisotropy field on the frequency of resonance,

$$H_0 = \frac{(f_0)_{Mc}}{2.8} \text{ oersted} \tag{13}$$

where $(f_0)_{Mc}$ is in megacycles. By (10), (12), and (13),

$$\Delta H = \frac{(f_0)_{Mc}}{5.6Q_e(A - 1)} \text{ oersted} \tag{14}$$

Since for strip-line and waveguide configurations, Q_e can be obtained directly from the information in Section III of this discussion, ΔH can be determined by measuring $(L_A)_{max}$ and then computing ΔH from (14).

The author found from discussions with Dr. K. L. Kotzebue (formerly of the Watkins-Johnson Co.) that he has frequently made linewidth measurements by making band-stop tests, then applying the approximate formula

$$\Delta H = \frac{(\Delta f)_{Mc/s}}{2.8A} \text{ oersted} \tag{15}$$

where $(\Delta f)_{Mc/s}$ is the bandwidth defined in Fig. 1 in megacycles, and A is given by (11). Equation (15) can be derived from (12), (13) above, and (8) of Kotzebue [14]. Because of certain approximations involved, this formula should be most accurate if $(L_A)_{max}$ is sizeable.

Dr. Kotzebue and the author made some trial tests and compared the two procedures just discussed. The results were in encouragingly good agreement. Table V shows the results of another series of tests on garnet spheres tested in standard X-band waveguide. The spheres were mounted in the guide by inserting them in a piece of polyfoam, which was slipped into the guide. No effort was made to orient the crystal axes in any special way. For each case, $(L_A)_{max}$ and Δf were measured, and ΔH was computed both by (14) and (15). Note that the two values of ΔH are, for the most part, in good agreement, especially when considering that the accuracy in measuring Δf was probably only to a few tenths of a megacycle.

The structure in Fig. 10 has also been used for testing ferrimagnetic resonators [15], and the results obtained were in reasonably close agreement with the manufacturer's measurements which were made in other ways. (Of course, only one resonator was used in the structure at a time for these tests.) This structure was found to be particularly useful for testing gallium-substituted YIG resonators which had relatively low saturation magnetization which made coupling to them relatively diffi-

TABLE V
RESULTS OF SOME LINEWIDTH TESTS ON YIG AND Ga-YIG SPHERES IN X-BAND WAVEGUIDE

Material	Sphere diameter (inches)	$(L_A)_{max}$ (dB)	Δf (Mc/s)	ΔH (14) (oersted)	ΔH (15) (oersted)
YIG	0.072	19.5	11.0	0.43	0.42
Ga-YIG $4\pi M_s =$ 920 gauss	0.071	10.5	6.7	0.71	0.71
YIG	0.049	11.6	3.5	0.35	0.33
YIG	0.049	11.6	3.0	0.35	0.28
YIG	0.041	7.7	3.5	0.44	0.52

cult, and which made tests at relatively low frequencies of interest.

Due to certain approximations involved, (15) can be expected to deteriorate in accuracy if $(L_A)_{max}$ is not sufficiently large (i.e., probably $(L_A)_{max}$ should be around 10 dB or more). Some experimental results suggest that (14) will also give better results if $(L_A)_{max}$ is around 10 dB or preferably larger (though the need for this has not been fully checked at this time). Thus, it is recommended that a waveguide or strip-line structure be used that will give a reasonably tight coupling between the sphere and the structure. (A Q_e value between 500 and 1000 is satisfactory at X-band for most cases.) In waveguide structures, reduced-height waveguide will be required in cases where the waveguide cross-sectional dimensions are very large compared to the sphere diameter, but caution should be taken that the height of the guide is not reduced so much that the close proximity of the metal walls degrades the unloaded Q of the garnet resonator. A guide height of three times the diameter of the sphere is probably safe. Similar considerations hold when making tests using strip-line structures. Caution should also be taken to ensure that tests are not made at frequencies where a spurious response is very close to the main response.

The two test procedures described above are both quite simple and easy to use, but the one based on (14) appears to be especially convenient, since it only requires that $(L_A)_{max}$ be measured (no bandwidth measurements are needed). As can be seen from Table V, the tests can be made in standard X-band waveguide for the more common sizes of YIG spheres, and no special test devices are required. Strip-line structures such as those in Figs. 2 or 5 can also be conveniently used. If the strip line and ground plane are too close to the resonator there may be some degradation of ΔH, as a result. However, if the resonator under test is to be used in a filter having similar strip-line dimensions, these results may be more practically meaningful than would be tests made in a special test structure having all metal walls far removed from the resonator under test.

VI. CONCLUSIONS

The experimental results obtained were seen to be in satisfactory agreement with the theory. In order to obtain a sufficiently large stop-bandwidth, for many applications special measures will be required in order to obtain sufficiently large coupling to the ferrimagnetic resonators. Use of dielectric loading is one possibility, but as evidenced by the tests on Filter 3, the use of shielding walls will be required for many cases where the resonators are spaced a quarter-wavelength at mid-tuning range. For a structure such as that in Fig. 5 it should be possible to design the shunt capacitors to serve as shielding walls, and structures of this type may well prove to be the most practical way to obtain large stop-band widths [with the relatively large value of $(L_A)_{max}$ that goes with a large stop-bandwidth]. To obtain best shielding between resonators, the shunt capacitors should probably be designed in a manner similar to the shielding walls in Fig. 10 (rather than as shown in Fig. 5 where the H-field might too easily couple through the horizontally oriented dielectric spacer pieces in the capacitor blocks).

The technique described for measuring the linewidth of ferrimagnetic resonators should be convenient for many workers.

ACKNOWLEDGMENT

The mechanical design of the filters discussed herein was worked out by York Sato, and he also conducted the laboratory tests. The structures were fabricated by C. A. Knight.

REFERENCES

[1] Lax, B., and K. J. Button, *Microwave Ferrites and Ferrimagnetics*, New York: McGraw-Hill, 1962.
[2] Carter, P. S., Jr., Magneticall tunable microwave filters using single-crystal yttrium-iron-garnet resonators, *IRE Trans. on Microwave Theory and Techniques*, vol. MTT-9, May 1961, pp 252–260.
[3] Young, L., G. L. Matthaei, and E. M. T. Jones, Microwave bandstop filters with narrow stop bands, *IRE Trans. on Microwave Theory and Techniques*, vol MTT-10, Nov 1962, pp 416–427.
[4] Harvard University, Radio Research Laboratory Staff, *Very High-Frequency Techniques*, vol. 2, New York: McGraw-Hill, 1947, pp 769–795.
[5] Matthaei, G. L., L. Young, and E. M. T. Jones, *Microwave Filters, Impedance-Matching Networks, and Coupling Structures*. New York: McGraw-Hill, 1964, ch 7.
[6] Cohn, S. B., Design relations for the wide-band waveguide filter, *Proc. IRE*, vol 38, Jul 1950, pp 799–803.
[7] Kotzebue, K. L., An electronically tunable band-reject filter, *1961 IRE WESCON*, paper 40/2.
[8] Matthaei, G. L., L. Young, and E. M. T. Jones, [5], ch. 4. See also: Weinberg, L., Additional tables for design of optimum ladder networks, *J. Franklin Inst.*, vol. 264, pt 1 and 2, Jul and Aug 1957, pp 7–23 and pp 127–138.
[9] Shiffman, B. M., P. S. Carter, Jr., and G. L. Matthaei, Microwave filters and coupling structures, SRI Project 3526, Contract DA 36-039 SC-87398, Seventh Quarterly Progress Rept, pt 3, Stanford Research Inst., Menlo Park, Calif., Oct 1962.
[10] Matthaei, G. L., L. Young, and E. M. T. Jones, [5], ch 6.
[11] Matthaei, G. L., L. Young, and E. M. T. Jones, *ibid.*, ch 17.
[12] Suhl, H., The nonlinear behavior of ferrites at high microwave signal levels, *Proc. IRE*, vol. 44, Oct 1956, pp 1270–1284.
[13] Matthaei, G. L., et al., Design criteria for microwave filters and coupling structures, Final Rept SRI Project 2326, Contract DA 36-039 SC-74862, Stanford Research Inst., Menlo Park, Calif., ch 28, Jan 1961.
[14] Kotzebue, K. L., Broadband electronically-tunable microwave filters, *1960 WESCON Conv. Rec.*, pt 1, pp 21–27.
[15] Matthaei, G. L., Novel microwave filter design techniques, Contract DA 36-039-AMC-00084(E), SRI Project 4344, Stanford Research Inst., Menlo Park, Calif., Quarterly Progress Rept 2, sec 3, Jul 1963.